Damage Evaluation in Freezing and Thawing Test of Concrete by Elastic-Wave Methods

Masayasu Ohtsu

Graduate School of Science and Technology

Kumamoto University, 2-39-1 Kurokami, Kumamoto 860-8555, Japan

Phone +81-96-342-3542, Fax. +81-96-342-3507, e-mail: ohtsu@gpo.kumamoto-u.ac.jp

Abstract:

In the freezing and thawing test of concrete, the frost damage is nondestructively evaluated by elastic-wave methods. In this regard, two alternative methods are recently proposed in RILEM recommendations. One is based on the ultrasonic test, which measures the transmission time of the longitudinal wave (P wave) and the other is associated with the resonant frequencies of vibrations. Re-examining formula to estimate dynamic moduli of elasticity in the standards available, evaluation of the frost damage by the elastic-wave methods is studied. Concerning the resonant frequencies of concrete samples, a three-dimensional analysis is performed by the boundary element method to identify actual vibrating-modes. It is clarified that an assumption of the one-dimensional resonant vibration is not applicable, because the assumption is responsible for a discrepancy between the dynamic and the static moduli. In order to evaluate the frost damage experimentally, the freezing and thawing tests were conducted by employing concrete samples after 1 year curing. The modulus of elasticity obtained from P-wave velocity is recommended to use as the durability factor, although homogeneous damages are only assumed in concrete samples. It is found that this modulus is comparable to the tangential modulus of elasticity in the compression test.

Key Words: Frost damage, Freezing and thawing, Modulus of elasticity, Resonance method, Boundary element method

1. Introduction

One RILEM recommendation [1] is recently published to determine the frost resistance of concrete to internal damage due to frost action. For nondestructive evaluation (NDE) of internal damage, two alternative methods A and B are standardized. The alternative method A is based on the ultrasonic test (UT), where the transmission time of the longitudinal elastic wave (P-wave) in a

concrete specimen is measured. In the conventional UT method, P-wave velocity is estimated from the transmission time, detecting elastic waves of the high frequency range over the audible sounds (ultrasonic waves). The alternative method B is associated with the test method for the fundamental transverse frequency in ASTM C215 [2], which is known as the resonant frequency (RF) method in a similar manner to the Japanese Standard: JIS A 1148 [3].

In addition to the measurement of changes in weight and length, these alternative methods A and B are to be available for evaluating the resistance of concrete subjected to rapid freezing and thawing. Since the changes in the length and the weight are essentially sensitive to scaling defects, the transmission time is the representative value in the alternative method A.

The both alternative A and alternative B methods physically belong to the elastic-wave methods. They are theoretically applicable to estimate accumulation of micro-cracks as the change of elastic moduli, although only homogeneous damage distribution could be taken into account. In the UT, the modulus of elasticity is reasonably determined from the velocity of P-wave. In the RF methods, dynamic moduli of elasticity are calculated from the resonant frequencies of longitudinal-vibration mode, bending (transverse)-vibration mode and torsional-vibration mode. The ratios of dynamic moduli of elasticity of damaged concrete to those of intact concrete are defined as the durability factor of concrete resistance to the frost damage [2].

On the basis of these alternative methods, formula for calculating the moduli of elasticity are studied. This is because the moduli calculated from the UT are sometimes not in good agreement with those of the RF method. In addition, it is reported that dynamic moduli of elasticity are greater static moduli, as the difference depends, in part, on the strength level of concrete. It is also noted that in the RF method, one-dimensional vibration is assumed, neglecting the effect of Poisson’s ratio.

In order to study a relation between the frost damage and the moduli of elasticity by the alternative methods, the rapid freezing and thawing tests in water were conducted. To study actual vibration modes in the RF method, three-dimensional (3D) dynamic analysis is performed by the boundary element method (BEM). Further, compression tests were carried out to estimate the static

modulus of elasticity. Thus, relative moduli estimated in the freezing and thawing tests are compared among results obtained from the transmission times in the UT, static moduli in the compression tests, and dynamic moduli in the RF methods.

2. Modulus of Elasticity

2.1 P-wave velocity

Elastic waves are generated and propagate in concrete, driving the impact force. In an isotropic, homogeneous and elastic body, the longitudinal wave (P-wave) propagates with the velocity v_p,

$$v_p = \sqrt{\frac{E(1-\nu)}{\rho(1-2\nu)(1+\nu)}}, \qquad (1)$$

where E is the modulus of elasticity, ν is Poisson's ratio and ρ is the density of concrete. In the UT, the transmission time of P-wave is measured and then the velocity is determined from dividing the travel distance by the transmission time. Thus, the modulus of elasticity, E_d, is determined from Eq. 1,

$$E_d = \rho v_p^2 \frac{(1-2\nu)(1+\nu)}{1-\nu} \quad . \qquad (2)$$

2.2 Resonant frequency of longitudinal vibration

In the RF method of longitudinal vibration, P-wave is assumed to propagate in an infinite bar, as Poisson's is set to be equal to zero in Eq. 1. Thus, we obtain,

$$v = \sqrt{\frac{E}{\rho}}. \qquad (3)$$

If we assume that Poisson's ratio = 0.2 in concrete, the coefficient $\{(1 - 2\nu)(1 + \nu)/(1 - \nu)\}$ in Eq. 1 is equal to 0.9. Accordingly, 10% difference in the dynamic modulus of elasticity between E (= ρv^2) obtained from Eq. 3 and E_d in Eq. 2 is readily derived.

In a test of the RF method, the fundamental longitudinal frequency of a specimen, f, is measured. A relationship between the wavelength l and the wave velocity v is derived as,

$$l = \frac{v}{f}. \qquad (4)$$

Assuming the longitudinal-vibrating mode of the specimen, the length of the specimen L is referred to as equal to a half of the wavelength as $l = 2L$ at the fundamental resonant frequency, and then we have a relation $v = 2Lf$ from Eq. 4. Eventually, the dynamic modulus of elasticity, E_D, in the RF method of the fundamental longitudinal vibration is obtained from Eq. 3,

$$E_D = \rho(2Lf)^2. \qquad (5)$$

2.3 Compression test

The static modulus of elasticity of concrete is usually estimated as a secant modulus of a stress-strain relation in a compression test, as a gradient between 1/3 point of the ultimate stress and an offset stress around 50 μ strain. Here, in order to determine a tangential modulus of elasticity systematically, continuum damage mechanics [4] is introduced. Damage scalar-parameter Ω in continuum damage mechanics is defined as a relative change in the modulus of elasticity, as follows,

$$\Omega = 1 - \frac{E}{E^*}, \qquad (6)$$

where E is the modulus of elasticity of a concrete specimen tested, and E^* is the modulus of intact and undamaged concrete. Loland introduced a relationship between the damage parameter Ω and strain ε under compression [5],

$$\Omega = \Omega_0 + A_0 \varepsilon^{\lambda}. \qquad (7)$$

As shown in Fig. 1 (a), Ω_0 is the initial damage at the onset of the compression test, and A_0 and λ are empirical constants. In the compression test, the damage is accumulated as a function of strain ε, and the damage parameter Ω increases from Ω_0 to Ωc as sown in the figure. It is noted that the effect of inhomogeneous damage distribution in the concrete specimen is also not taken into account in the model.

In the freezing and thawing test, the initial damage Ω_0 is assumed to homogeneously increase with the increase in the freeze-thaw cycles. Substituting Eq. 7 into Eq. 6, the following stress-strain (σ-ε) relation is derived,

$$\sigma = E\varepsilon = E^*(1-\Omega)\varepsilon = E^*(1-\Omega_0 - A_0\varepsilon^{\lambda})\varepsilon = E_0\varepsilon - E^*A_0\varepsilon^{\lambda+1}, \quad (8)$$

where $E_0 = E^*(1 - \Omega_0)$.

In the compression test, a relation between stress and strain is obtained as shown in Fig. 1(b). From Eq. 8, it is easily understood that the initial modulus of elasticity E_0 corresponds to a tangential modulus. The modulus of elasticity varies from the initial E_0 to the final *Ec*. It is noted that the latter is a secant modulus as $\sigma_c = Ec\ \varepsilon_c$, where σ_c and ε_c are the strength and the ultimate strain, respectively. The initial modulus of elasticity E_0 is to be determined as a tangential gradient of the stress-strain curve. Consequently, a stress-strain relation was approximated by Eq. 8, carrying out the multi-regression analysis for three variables E_0, E^*A_0 and λ. Then, the static modulus, E_0, was determined as a tangential modulus when $d\sigma/d\varepsilon$ at $\varepsilon = 0$.

3. Experiment

3.1 Specimens

Mixture proportion and properties of flesh concrete are given in Table 1. The maximum gravel size is 20 mm. Specific gravities of gravel and sand are 3.07 and 2.63, respectively, in the surface-dry and saturated condition. To minimize the effects of scaling and deterioration at the surface zone in the freezing and thawing test, air content was kept over 4 %, employing an admixture. Eight prismatic specimens of dimensions 100 mm x 100 mm x 400 mm and three cylindrical specimens of 100 mm diameter and 200 mm length were made. In order to circumvent the effect of curing in the freezing and thawing process, all the specimens were cured for one year in the controlled room with RH 60% and 20^o Celsius, following the 28 day water-curing in a water reservoir (20^o Celsius). It was expected that 1 year-curing might lead to minor damages of concrete specimens in the freezing and thawing process. The cases of low- deteriorated concrete are to be studied, because concrete properties, in particular, near the surface is even better than those of 28 day-cured concrete due to hydration reaction.

Six specimens were deteriorated by freeze-thaw cycles in water, as standardized in ASTM C666 [6]. During one cycle, temperature was varied from -18^o Celsius to 5^o Celsius for three to four hours. Two specimens damaged

by 100 cycles, 200 cycles, and 300 cycles were prepared. For 0 cycles, two specimens were stored simply in the controlled room until the test.

3.2 Elastic-wave methods

During the freezing and thawing tests, the transmission time of P-wave was measured in the axial direction, by using a UT device (SIT-021, Sanwa Co.) as shown in Fig. 2 (a). The axial length of the specimen was precisely measured. Then, as the averaged value of the two specimens, P wave velocity was determined at 0 cycles, 100 cycles, 200 cycles and 300 cycles.

Following the UT measurement, fundamental resonant frequencies of the specimens were determined in two specimens. Although the dynamic modulus of elasticity E_D was only estimated from the longitudinal vibration by Eq. 5, fundamental resonant frequency of the transverse (bending) vibration was also determined in the RF method. The device (Model MIN-011-8, Marui Co.) and a test set-up are illustrated in Figs. 2 (b) and 2 (c). By employing a sweep-mode drive (auto-scanning), the resonant frequencies were estimated from the peak frequencies of spectral responses (frequency spectra). The responses were calibrated by compensating the system response, which was measured by the face-to-face of the input and output sensors, prior to the tests.

3.3 Compression test

After the measurements in the UT and the RF method, each specimen was cut into two prismatic specimens of dimensions 100 mm x 100 mm x 200 mm. Then, compression tests were conducted. Two strain gauges of 70 mm were pasted in the axial direction to measure axial strains.

Prior to the freezing and thawing tests, compressive strength of concrete at one-year age was determined as the averaged value of three cylindrical specimens. The compressive strength of concrete at 1 year age was 46.2 MPa.

4. BEM Analysis

A three-dimensional (3D) boundary element model analyzed is illustrated in Fig. 3. The boundary element method (BEM) is a numerical technique to solve a elastic body with only the boundary conditions [7]. Assuming an isotropic, homogeneous and elastic medium, an integral equation of Navier's equilibrium

equation is derived on the basis of Gauss's integral formulas, and is analyzed numerically by dividing the boundary surfaces into boundary meshes. In order to solve frequency responses of specimens, Navier's equation was transformed into the frequency domain and the integral equation in the frequency domain was solved. Under a particular frequency with 1 N force at the input point, deformations at the surface of the specimen were determined. Corresponding to the RF method, input and output points were arranged for the longitudinal and the bending vibrations, respectively. Thus, the vertical deformation at the output point at the particular frequency was obtained and plotted against the frequency as a frequency spectrum. In Fig. 3, an input point for the torsional vibration is also denoted, although results are out of the scope here.

The size of a boundary mesh was 50 mm x 50 mm for the longitudinal vibration, while that is set to 20 mm x 20mm for the bending vibration because of the supporting conditions. These could affect numerical results in the high frequency range. To construct the frequency spectrum, which was detected at the output point, frequency varies with 100 Hz increment from 0 to 20 kHz. The dynamic moduli of elasticity for computation were estimated from Eq. 3 after freeze-thaw cycles, measuring the velocities of P wave and the densities. These values are summarized in Table 2. Poisson's ratio was always set to be equal to 0.2, not taking dynamic Poisson's ratio into consideration. Later, it is clarified that there is no difference between the dynamic and the static properties.

It is noted that all results of the BEM analysis are obtained, assuming a homogeneous body. Concrete damages, however, in the freezing and thawing tests should be referred to as inhomogeneous. Here, results of the elastic moduli obtained by the elastic-wave methods are mainly discussed. They are derived from the assumption of one-dimensional (1D) and a homogeneous body, because the fundamental resonance is taken into consideration. It is known that the effect of inhomogeneity could affect seriously in the higher resonant frequencies. Because the vibration-modes of the fundamental resonant frequency are studied, results of the BEM analysis are useful to discuss a difference between 3D and 1D vibrations.

5. Results and Discussion

5.1 Spectral responses in the resonance method

A spectral response (spectrum) of the longitudinal vibration at 0 cycle in the test is compared with that of the BEM analysis in Fig. 4. The former in the test has three particular peaks, while that of the latter has many peaks, in particular, in the higher frequency range. It could be the effects of mesh division and supporting conditions of the model, because these effects are emphasized in the higher frequency range. It is still observed that the fundamental (1^{st}) resonant frequency of the test is in good agreement with that of the BEM analysis.

Similarly results at 300 cycles elapsed are given in Fig. 5. It is observed that the number of the peak frequencies in the BEM analysis further increase and the frequency response is quite complicated, while only three peaks are again observed in the test. Still, agreement between the 1^{st} resonance frequency of the test and that of the BEM analysis is reasonably good. It is obviously observed that these resonant frequencies in Fig. 5 are lower than those of Fig. 4 due to damage accumulation. Because the effect of inhomogeneous damage evolution is not taken into account in the BEM analysis, many peak frequencies observed should be associated with reflections of elastic waves and the supporting conditions, without attenuation due to frost damage. In contrast, the effect of inhomogeneous damage may affect the frequency spectrum of the test at 300 freeze-thaw cycles. But, the difference between the spectra at 0 cycles and at 300 cycles is minor, as peak frequencies are observed only at slightly lower frequencies. This may suggest that the effect of inhomogeneous damage is not emphasized in the low frequency range up to 20 kHz.

A frequency spectrum of the transverse vibration at 300 cycles is compared with that of the BEM analysis in Fig. 6. The 1^{st} resonance of the transverse vibration is again in reasonable agreement with that of the BEM analysis.

Since the peak frequencies in the higher frequency range are possibly dependent on the mesh division and the supporting condition, the 1^{st} resonant frequencies are only compared between the RF method and the BEM analysis. Results are summarized in Table 3. Agreement is reasonably good as the differences are within 1.5 %. Thus, it is demonstrated that the 1^{st} resonant frequencies observed in the tests are successfully reproduced by the BEM analysis.

As a result, it is considered that the effect of inhomogeneous damage evolution in the freezing and thawing tests is minor in respect with the fundamental frequencies.

5.2 Vibrating modes

Since the 1st peak-frequencies observed in the RF method are found to be reasonably close to those of the BEM analysis, vibrating modes obtained in the BEM analysis are studied.

A three-dimensional (3D) vibrating modes of the longitudinal vibration at 300 cycles are illustrated in Fig. 7. Displacements analyzed are magnified to easily figure deformations out. It is found that the vibrating mode is not of simple extension-compression mode as assumed in the RF method, because the concrete specimen is not an infinitely long bar, but a finite prismatic bar. In order to clarify the difference from the one-dimensional (1D) deformation, displacements at the middle cross-section is illustrated in Fig. 8. All displacements are relatively magnified. 1D deformation is drawn as just containing the outer boundary of 3D deformation. It is found that 3D deformation is not similar to 1D deformation. This suggests that estimation of the wave velocity by Eq. 3 is not rational, because the vibrating modes are not simply longitudinal. It could be, in part, a reason why P-wave velocities estimated by Eq. 3 are generally higher than those estimated by the UT.

3D vibrating mode of the transverse vibration at 300 cycles is given in Fig. 9. It is observed that a deformation at the top surface is simply of bending mode, while the bottom boundary (surface) bends upwards due to the effect of input force. So, the deformation at the middle cross-section is compared with the simple bending mode in Fig. 10. It is realized that the difference between 1D deformation and 3D deformation at the top surface is small, while 3D deformation at the bottom surface is far different from 1D deformation of the bending mode. Because an output sensor is normally set at the top surface, it is considered that a difference between 1D and 3D deformations is negligible in the transverse vibration. It is noted that the frost damage normally penetrates from the surface and thus the damaged layer is created near the surface. Accordingly, this might not be the case of heavily damaged concrete in the freeze-thaw process.

5.3 Modulus of Elasticity

The dynamic modulus of elasticity, E_D, estimated by the RF method is calculated on the basis of the 1D vibration as formulated $v = 2Lf$. In the case, the dynamic modulus is not identical to the modulus by Eq. 2, neglecting the effect of Poisson's ratio. Thus, P-wave velocity estimated from the RF method could become higher than the measured values in the UT. From the vibrating modes, it is demonstrated that the deformations are not simply of the 1D motion.

It is reported that the dynamic modulus is greater than the static modulus. This could result from the static modulus of elasticity, determined by the secant modulus to be estimated in the compression test. This is a reason why the difference between the dynamic and static moduli depends on the strength level of concrete. Consequently, the static modulus of elasticity, E_0, was obtained from Eq. 8 as a tangential modulus. The strengths and the static (tangential) moduli obtained after the freezing and thawing tests are summarized in Fig. 11. Since air content is over 4 %, the decreases of the strengths and moduli seem to be not remarkable due to low deterioration.

The modulus of elasticity E_d was determined by Eq. 2 in the UT measurement. Here P-wave velocity was determined, the density was measured, and Poisson's ratio was assumed as 0.2. Comparison between the tangential moduli E_0 and the dynamic moduli E_d is given in Fig. 12. The static (tangential) moduli of elasticity are in reasonable agreement with the dynamic moduli. These results demonstrate that there exist no difference between the static (tangential) modulus of elasticity in the compression test and the dynamic modulus estimated from P-wave velocity.

5.4 Damage Evaluation

In a similar manner to the damage factor in ASTM C666 [6], the JIS A 1148 code [3] and the alternative method B in RILEM recommendation [1] state that the damage due to freezing and thawing is estimated as the relative modulus, which is estimated from the decrease in the peak frequency in the bending vibration,

$$P_{bend} = [f_n/f_0]^2 \text{x} 100, \qquad (9)$$

where f_n is the peak-frequency in the bending vibration at n freeze-thaw cycles and f_0 is the peak-frequency at 0 cycle. In principle, the relative modulus defined by Eq. 9 is equivalent to that of the longitudinal vibration.

Consequently, from the ratio of the 1st resonant frequencies in the longitudinal vibration, a similar parameter P_{long} is derived.

From Eq. 2, it is found that the relative modulus is equivalently obtained from the velocity of P wave. Thus, another parameter is estimated as,

$$V = [v_{pn}/v_{p0}]^2 \times 100, \quad (10)$$

where v_{pn} is the velocity of P wave in the UT after n freeze-thaw cycles, and v_{p0} is the velocity at 0 cycle.

Above-mentioned parameters are obtained as relative moduli, they are directly estimated as the ratio of static moduli as,

$$E = E_{0n}/E_{00} \times 100. \quad (11)$$

Here E_{0n} is the static (tangential) modulus of elasticity in the compression test after n freeze-thaw cycles and E_{00} is the modulus at 0 cycle.

These damage parameters are compared in Fig. 13. When taking the ratios as relative values, the differences among the relative moduli are not appreciable. So, it is considered that the difference between the alternative methods A and B is practically not crucial. It is found that relative moduli by the bending vibration are the lowest. This may suggest the presence of damaged layer near the surface as inhomogeneous damage. Thus, relative moduli by the longitudinal vibration are slightly larger than those of the bending vibration, because the longitudinal vibration is not sensitive to local damage. As could be expected, relative moduli by P-waves are almost identical to those of static (tangential) moduli. Thus, the alternative method A could result in a comparable estimation to the static modulus of elasticity.

6. Conclusion

For estimation of the internal damage in concrete subjected to freezing and thawing, the UT and the RF method are investigated. Results are summarized, as follows:

(1) Velocities determined from the fundamental resonant frequencies of the longitudinal vibration in the RF method become faster than the measured velocities by the UT, because of one-dimensional assumption.

(2) By the BEM analysis, vibration modes at the fundamental frequencies are analyzed. The longitudinal vibrations are not of simple one-dimensional motion. This could leads to the fact that the modulus of elasticity E_D

estimated from the RF method is larger than E_d of the UT.

(3) For the bending vibration, the difference between 1D and 3D deformations is not so large as observed in the longitudinal vibration. However, since the frost damage normally progresses from the surface, the damaged layer created near the surface could affect the resonant vibrations.

(4) The static modulus of elasticity is obtained as a tangential modulus in the compression test, while the dynamic modulus of elasticity is determined from the velocity estimated by UT. No difference is physically found between the static moduli of elasticity and the dynamic moduli.

(5) Within the very low deterioration of the concrete investigated, the difference between the frost damages estimated by the alternative methods A and B is practically not crucial. The relative modulus determined from the wave velocity in the UT (alternative method A) could be a reasonable parameter for the frost damage, because the modulus is comparable to the static modulus of elasticity.

ACKNOWLEDGEMENT

The research conducted is supported by Kumamoto University Global COE (Center of Excellence) Program: Global Initiative Center for Pulsed Power Engineering. To perform experiments and analyses, assistances of former graduate students: Messrs. Naoki Gotoh and Shou Noguchi are very valuable. The author wishes to deeply thank the program and their supports.

References

1. RILEM TC 176-IDC Final Recommendation (2004) Test Methods of Frost Resistance of Concrete: CIF-Test: Capillary Suction, Internal Damage and Freeze Thaw Test – Reference Method and Alternative Methods A and B, Materials and Structures, 37(274), 743-753.

2. ASTM C215-08 (2008) Standard Test Method for Fundamental Transverse, Longitudinal, and Torsional Frequencies of Concrete Specimens.

3. JIS A 1127 (2001) Japanese Industrial Standard Method of Test for Dynamic Modulus of Elasticity, Rigidity and Poisson's Ratio of Concrete by Resonance Vibration,

4. Loland, K.E.(1989) Continuous Damage Model for Load-Response Estimation of Concrete, Cement and Concrete Research, 10, 395-402.

5. Shah, S. P., Swarts, S. E., Ouyang, C. S. (1995) Fracture Mechanics of Concrete, John Wiley&Sons, Inc.New Yok, 452-462
6. ASTM C666 (2008) Standard Test Method for Resistance of Concrete to Rapid Freezing and Thawing.
7. Banerjee, P. K. and Shaw R. P. eds., Development of Boundary Element Methods -2, Applied Science Publishers, 1982.

Captions of tables and figures

Table 1 Mixture proportion of concrete and properties of flesh concrete

Table 2 Mechanical properties of concrete for BEM analysis

Table 3 Comparison of the 1st resonant frequencies

Fig. 1 Damage parameter Ω and moduli of elasticity *E*.

Fig. 2 (a) Measurement of P-wave velocity in the ultrasonic test, and tests of the resonance method for (b) longitudinal and (c) bending vibrations.

Fig. 3 BEM model for the resonance method.

Fig. 4 Frequency responses in the longitudinal vibration of the resonance method in (a) the test and (b) BEM analysis at 0 cycle freeze-thaw.

Fig. 5 Frequency responses in the longitudinal vibration of the resonance method in (a) the test and (b) BEM analysis at 300 cycle freeze-thaw.

Fig. 6 Frequency responses in the transverse vibration of the resonance method in (a) the test and (b) BEM analysis at 200 cycle freeze-thaw.

Fig. 7 3D vibrating mode at the 1st resonant frequency for the longitudinal vibration after 300 freeze-thaw cycles.

Fig. 8 Comparison between 3D deformation and 1D deformation in the longitudinal vibration.

Fig. 9 3D vibrating mode at the 1st resonant frequency for the transverse vibration after 300 freeze-thaw cycles.

Fig. 10 Comparison between 3D deformation and bending deformation in the transverse vibration.

Fig. 11 Strengths and static moduli of elasticity (tangential).

Fig. 12 Comparison between static moduli and dynamic moduli of elasticity in the resonance metnod.

Fig. 13 Comparison of relative moduli obtained in the freez-thaw tests.

Table 1 Mixture proportion of concrete and properties of flesh concrete

Max. gravel size (mm)	Water to cement ratio: W/C (%)	Weight per volume (kg/m^3)				Air content (%)	Slump (cm)
		W	C	S	G		
20	55	180	327	775	1142	4.5	4.9

Table 2 Mechanical properties of concrete for the BEM analysis

cycles	V_P (m/s)	E_d (GPa)	ρ (kg/m^3)
0	4250	40.6	2490
100	4180	38.8	2470
200	4110	37.3	2450
300	4080	36.4	2430

Table 3 Comparison of the 1st resonant frequencies

Vibrating modes	Freeze-thaw cycles	1st resonant freq. of the resonance method: f_{exp} (Hz)	1st resonant freq. of the BEM analysis: f_{ana} (Hz)	Difference : f_{ana}-f_{exp}/f_{exp} x 100 (%)
Longitudinal vibration	0	5440	5480	0.74
	100	5390	5385	-0.09
	200	5320	5300	-0.38
	300	5240	5255	0.29
Bending vibration	0	2350	2315	-1.49
	100	2290	2275	-0.66
	200	2260	2240	-0.88
	300	2210	2200	-0.45

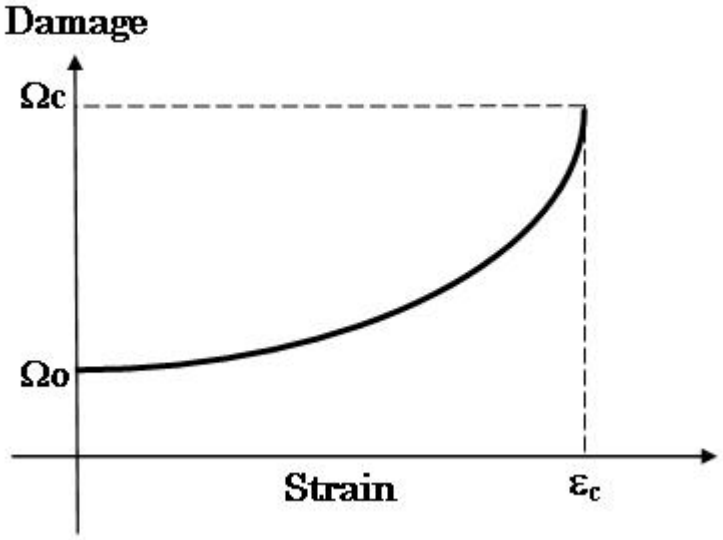

(a) Damage evolution in the compression test.

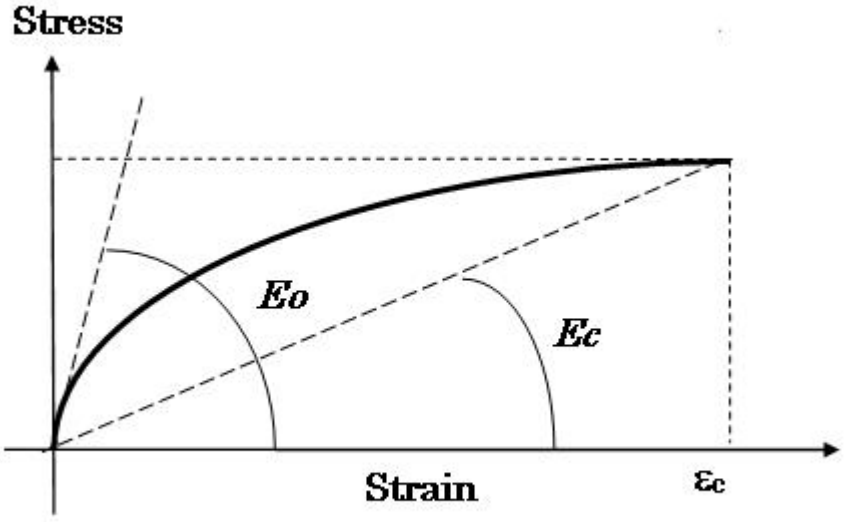

(b) Stress-strain relation

Fig. 1 Damage parameter Ω and moduli of elasticity *E*.

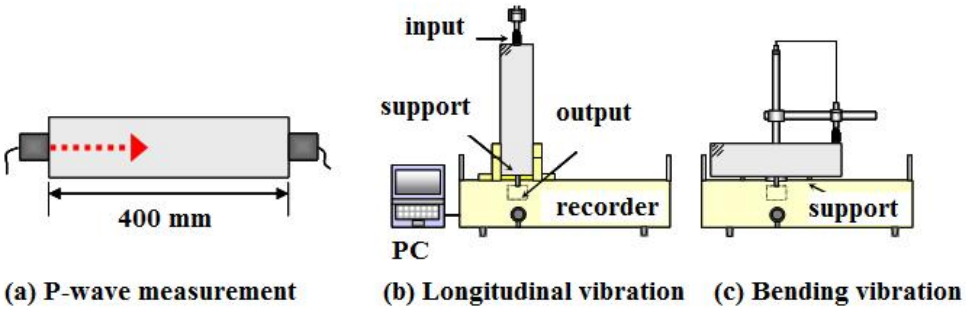

Fig. 2 (a) Measurement of P-wave velocity in the UT, and test set-ups of the resonance method for (b) longitudinal and (c) bending vibrations.

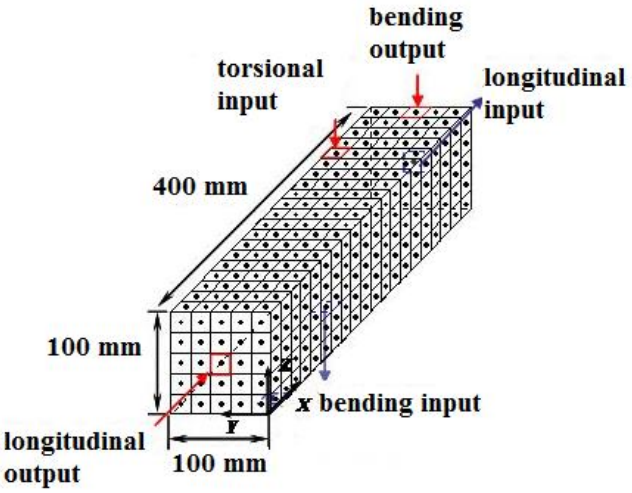

Fig. 3 BEM model for the resonance method.

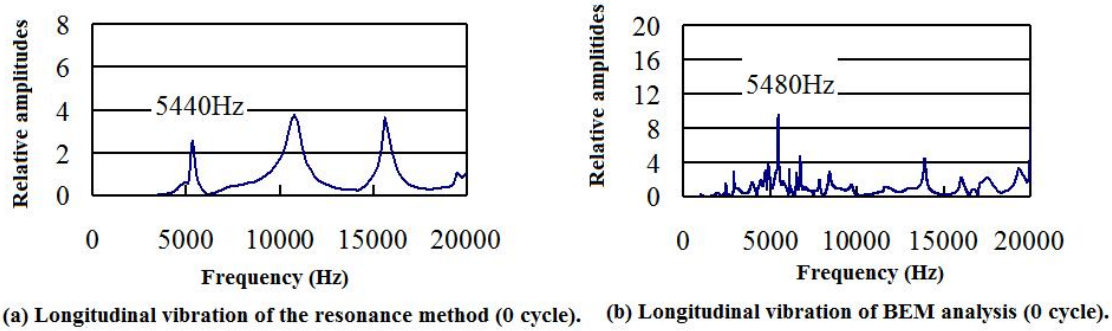

Fig. 4 Frequency responses in the longitudinal vibration of (a) the resonance method and (b) the BEM analysis at 0 freeze-thaw cycle.

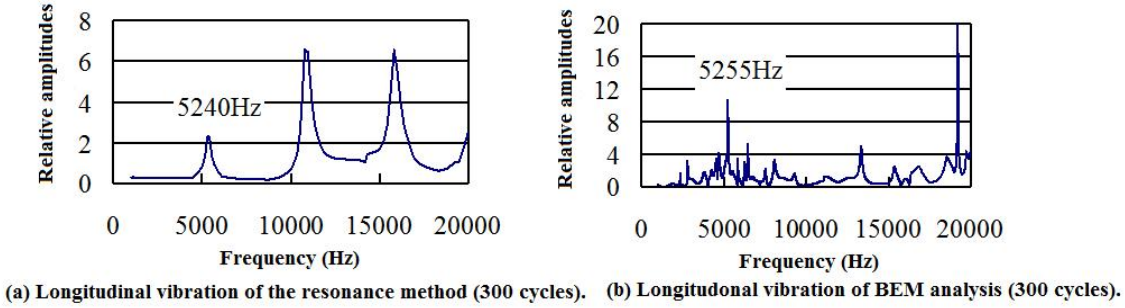

Fig. 5 Frequency responses in the longitudinal vibration of (a) the resonance method and (b) the BEM analysis at 300 freeze-thaw cycles.

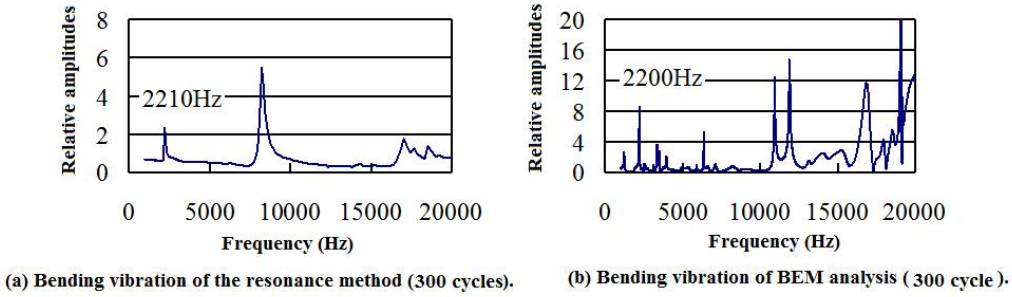

Fig. 6 Frequency responses in the transverse vibration of (a) the resonance method and (b) the BEM analysis at 300 freeze-thaw cycles.

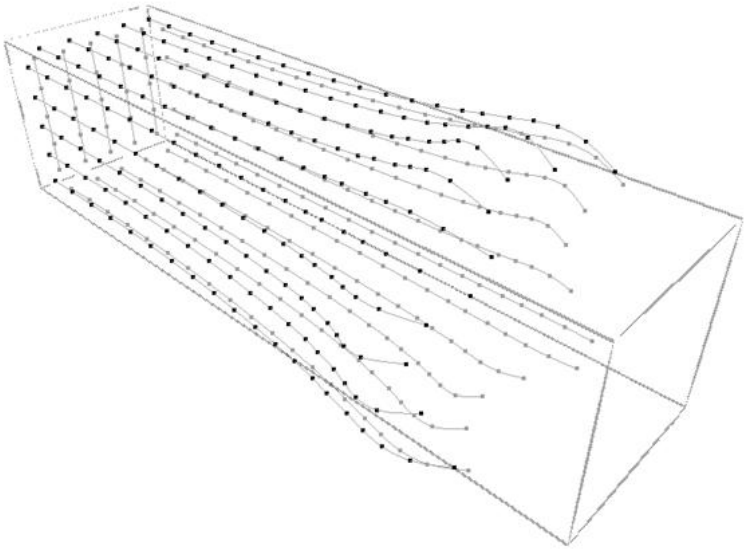

Fig. 7 3D vibrating mode at the 1st resonant frequency for the longitudinal vibration at 300 freeze-thaw cycles.

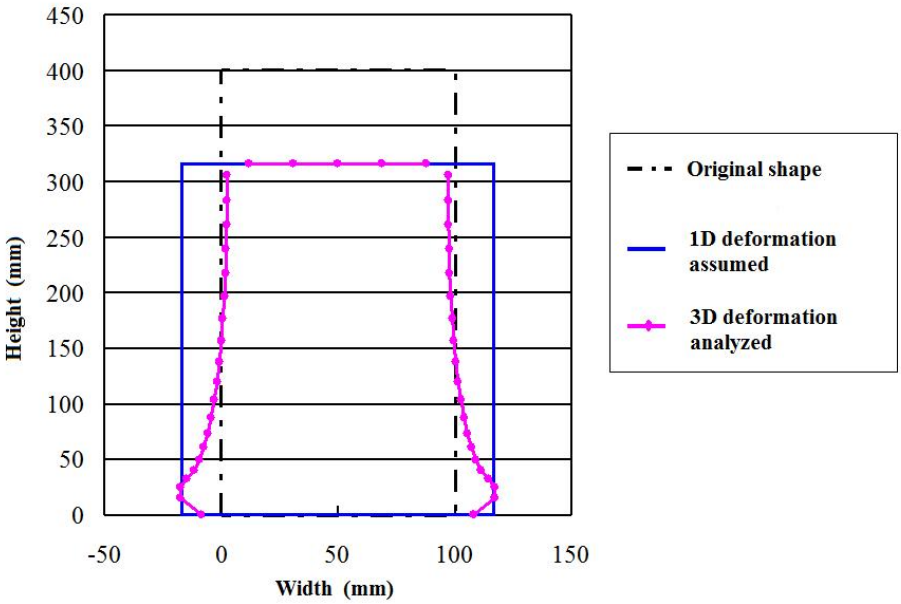

Fig. 8 Comparison between 3D deformation (analyzed) and 1D deformation (assumed) in the longitudinal vibration at 300 freeze-thaw cycles.

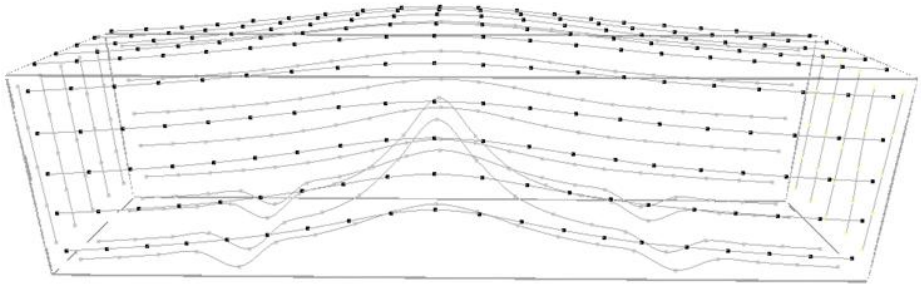

Fig. 9 3D vibrating mode at the 1st resonant frequency for the transverse vibration after 300 freeze-thaw cycles.

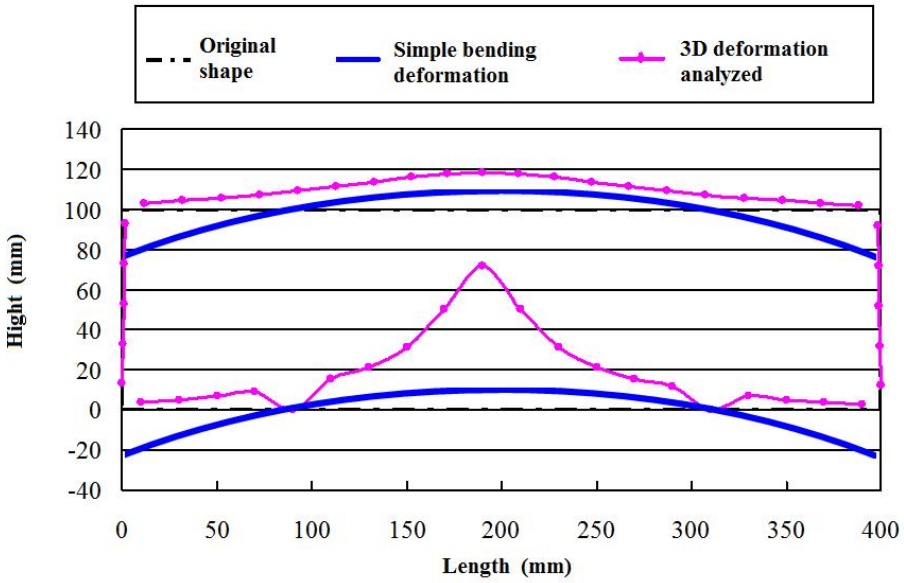

Fig. 10 Comparison between 3D deformation (analyzed) and a simple bending deformation in the transverse vibration at 300 freeze-thaw cycles.

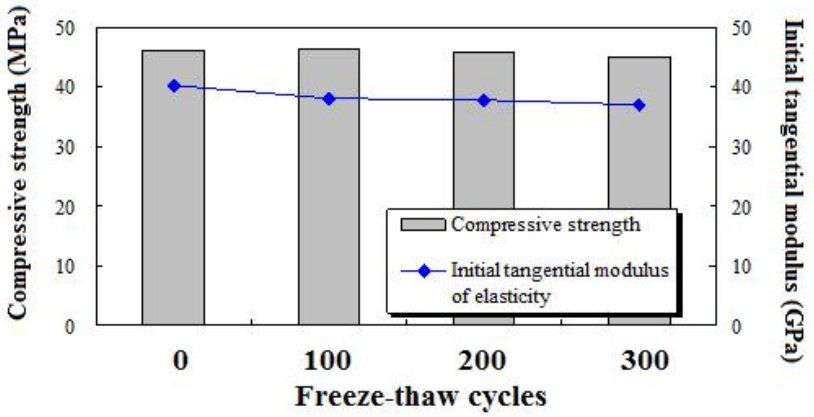

Fig. 11 Strengths and static moduli of elasticity (tangential) in the freezing and thawing tests.

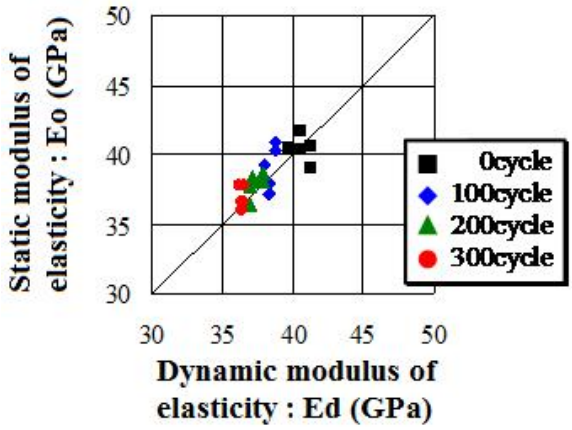

Fig. 12 Comparison between static (tangential) moduli and dynamic moduli of elasticity by P-wave velocities in the freezing and thawing tests.

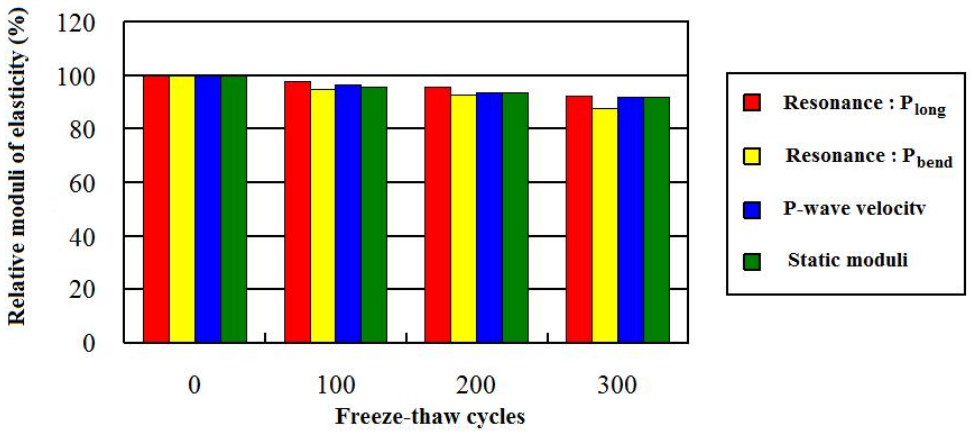

Fig. 13 Comparison of relative moduli obtained in the freezing and thawing tests.